

SCIENTIFIC REPORTS



OPEN

Large-area growth of multi-layer hexagonal boron nitride on polished cobalt foils by plasma-assisted molecular beam epitaxy

Zhongguang Xu, Hao Tian, Alireza Khanaki, Renjing Zheng, Mohammad Suja & Jianlin Liu

Received: 05 August 2016
Accepted: 18 January 2017
Published: 23 February 2017

Two-dimensional (2D) hexagonal boron nitride (h-BN), which has a similar honeycomb lattice structure to graphene, is promising as a dielectric material for a wide variety of potential applications based on 2D materials. Synthesis of high-quality, large-size and single-crystalline h-BN domains is of vital importance for fundamental research as well as practical applications. In this work, we report the growth of h-BN films on mechanically polished cobalt (Co) foils using plasma-assisted molecular beam epitaxy. Under appropriate growth conditions, the coverage of h-BN layers can be readily controlled by growth time. A large-area, multi-layer h-BN film with a thickness of 5–6 nm is confirmed by Raman spectroscopy, scanning electron microscopy, X-ray photoelectron spectroscopy and transmission electron microscopy. In addition, the size of h-BN single domains is 20–100 μm . Dielectric property of as-grown h-BN film is evaluated by characterization of Co(foil)/h-BN/Co(contact) capacitor devices. Breakdown electric field is in the range of 3.0–3.3 MV/cm, which indicates that the epitaxial h-BN film has good insulating characteristics. In addition, the effect of substrate morphology on h-BN growth is discussed regarding different domain density, lateral size, and thickness of the h-BN films grown on unpolished and polished Co foils.

Two-dimensional (2D) hexagonal boron nitride (h-BN) has received a great deal of attention due to its remarkable properties^{1–4}, such as large band gap (~6.0 eV), high thermal conductivity, excellent thermal and chemical stability, and its significant potential as an indispensable dielectric layer of building blocks in high-performance 2D integrated electronics and photonics^{5–10}. Among those efforts, 2D h-BN, which has a small lattice mismatch (1.7%) with graphene, and an atomically smooth surface that is relatively free of dangling bonds and trapped charges⁵, has been recently demonstrated to be an ideal encapsulation for graphene and other 2D materials^{8,11–15}. In addition, h-BN has been used as a gate dielectric to greatly enhance the performance of graphene electronics^{5,10,16}. To realize the technological potential of h-BN, it is essential to synthesize large-area, high-quality h-BN thin films through a scalable and controllable method. So far, tremendous efforts have been made to obtain large-area and high-quality h-BN films. Mechanical cleavage¹⁷ and liquid exfoliation¹⁸ can provide micrometer-sized, atomic-layer-thick h-BN flakes, but they are not suitable for large-area production due to the difficulty of controlling the thickness and size of the materials. Much progress has been made by chemical vapor deposition (CVD) of h-BN growth on various substrates, including Cu^{4,19–21}, Ni^{22,23}, Fe^{11,24}, Ru²⁵ and Pt^{26,27}. In addition, other methods, such as physical vapor deposition (pulsed laser deposition²⁸, reactive magnetron sputtering²⁵, ion beam sputtering deposition^{21,29}) and co-segregation^{30,31}, have been attempted. Nevertheless, there is still much to be done in each one of these methods in order to controllably and scalably synthesize high-quality h-BN thin films.

Most recently, molecular beam epitaxy (MBE) has been used to synthesize h-BN films on cobalt (Co) thin film and nickel (Ni) foil substrates^{32–34}. As an alternative approach to other methods, MBE can provide precise control over the growth conditions thanks to its ultra-high vacuum environment, atomic layer epitaxy accuracy and controllability, instant introduction and control of multiple sources, ease of doping of materials and *in-situ* layer-by-layer characterization. In addition, MBE is promising for the *in-situ* growth of vertically stacked

Quantum Structures Laboratory, Department of Electrical and Computer Engineering, University of California, Riverside, California 92521, USA. Correspondence and requests for materials should be addressed to J.L. (email: jianlin@ece.ucr.edu)

heterostructures with defect-free interfaces³⁵, which can bring about new opportunities to develop integrated 2D nanoelectronics, nanophotonics and spintronics³⁶. On the other hand, although h-BN has been grown on Ni foils by MBE^{33,34}, the growth mechanism remains elusive, moreover, no electrical and dielectric properties of those MBE grown h-BN films have been evaluated. In this paper, we report MBE growth of large-area, multi-layer h-BN films on polished Co foils for the first time. The growth mechanism is discussed based on the effect of substrate surface morphology on h-BN growth, and electrical and dielectric properties are characterized.

Experiments

A re-designed Perkin-Elmer MBE system was used for sample growth. A Knudsen effusion cell filled with B₂O₃ powder (Alfa Aesar, 99.999%) was used as boron (B) source. Nitrogen plasma (Airgas, 99.9999%) generated by an electron cyclotron resonance (ECR) system and high-purity ammonia (American Gas Group, 99.9995%) were used as nitrogen (N) sources (Supporting Information).

Co foils (0.1 mm thick, 99.995%) from Alfa Aesar were cut into 1 cm × 1 cm pieces as substrates. These pieces were degreased with acetone and IPA and rinsed in deionized (DI) water prior to use. Besides these unpolished substrates, polished substrates were mainly used in this experiment. The Co foil surface polishing was performed on an SBT 920 Lapping and Polishing workstation (details in Supporting Material). These Co foil substrates were cleaned with diluted hydrochloric acid (10%) to remove residual native oxide layer, rinsed with DI water, blown dry, and immediately loaded into the MBE chamber. The substrates were heated to 850 °C and annealed at this temperature under a 10-sccm (standard cubic centimeters per minute) flow of hydrogen gas for 10 minutes. Then, h-BN growth was started at the same substrate temperature. During the growth, B cell temperature was maintained at 1150 °C; N₂ gas flowed at 5 sccm through an ECR source, and NH₃ gas at a flow rate of 5 sccm was also introduced to the chamber through a needle valve. The ECR current was set at 60 mA with a power of 228 W, and the growth took 900 s for a reference sample on an unpolished Co foil (Sample A), and 450 s, 900 s and 1800 s on polished Co foils for Samples B, C, and D, respectively. Finally, the samples were cooled to room temperature at a rate of 10 °C/min. Table S1 (Supporting Materials) gives a summary of the growth conditions.

Raman characterizations were performed using a HORIBA LabRam system equipped with a 50-mW, 532-nm green laser. Scanning electron microscopy (SEM) images were acquired using an XL30-FEG SEM system. X-ray photoelectron spectroscopy (XPS) characterization was conducted using a Kratos AXIS ULTRA XPS system equipped with an Al K α monochromatic X-ray source and a 165-mm mean radius electron energy hemispherical analyzer. Atomic force microscopy (AFM) images were obtained using a Veeco D5000 AFM system. Transmission electron microscopy (TEM) images and selected area electron diffraction (SAED) patterns were acquired using a FEI Titan Themis 300 STEM. Plan-view TEM sample was prepared using a PMMA-assisted transfer method. After spin-coating with PMMA, the sample was submerged in FeCl₃ solution to etch away the Co metal layer. The film was then transferred onto a carbon-coated Cu TEM grid and treated with acetone and DI water to remove the PMMA. Samples transferred onto SiO₂-coated Si substrates were obtained using the same PMMA-assisted method.

Co(foil)/h-BN/Co(contact) capacitor devices were fabricated by a standard photolithography and lift-off process. A Co layer of 100 nm was patterned as top square contacts with an edge length of 20 μ m, 50 μ m and 100 μ m on the surface of as-grown h-BN film. Reactive ion etching (RIE) was performed with a 50-sccm SF₆ plasma, under a power of 50 W, and for 15 seconds to etch the h-BN film between devices, which ensured isolation of different devices on the same substrate. The current-voltage (I-V) characteristics were obtained by an Agilent 4155 C semiconductor parameter analyzer equipped with probing tips having a diameter of 5 μ m (Signatone, SE-TL).

Results and Discussion

Both unpolished and polished Co foils were used as substrates. The substrate cleaning, treatment and polishing procedures are described in the Experimental section in detail. The surface morphology comparison between unpolished and polished Co foils is shown in Figure S1, and discussed in the Supporting Material. Within a scanned area of 50 × 50 μ m², the root mean square (RMS) roughness of the polished Co foil is about 11 nm, compared to 231 nm for the unpolished Co foil. Figure 1 shows SEM images of the four as-grown samples (additional SEM images in Figure S2). All samples show h-BN features that are darker than their substrates in the images. White triangular h-BN domains are also observed on Sample A, which was grown on unpolished Co (Fig. 1a). The inset of Fig. 1a shows a magnified SEM image of a typical white triangle, which should be multilayer h-BN stacks^{21,24}. This result suggests that the MBE growth of h-BN is not self-limited²¹. Wrinkles are also evident on the surface, which represent the conformal growth of the film across very rough Co surface with ridges and valleys. In other words, these wrinkles are not induced by thermal strain effect as often observed from those films produced by fast substrate cooling³⁷ because we used very low cooling rate, the stress originated by different thermal expansion coefficients between the film and substrate can be readily relaxed without causing the formation of wrinkles. This is further proved for the films on polished samples where no wrinkles are observed. For the samples grown on polished Co, as the growth time increases from 450 s to 1800 s, the morphology of h-BN film evolves from discrete flakes into continuous film, as shown in the SEM images in Fig. 1b–d. At a growth time of 450 s, Sample B exhibits sparse h-BN flakes in random domain orientations with various edge sizes from a few micrometers to a few tens of micrometers (up to 40 μ m), which indicates that the nucleation sites are constantly formed and the initially formed smaller seeds grow into larger domains as the growth time elapses. Longer growth time of 900 s led to denser and relatively larger h-BN flakes, as well as conjoined h-BN domains (Figure S2c) on Sample C. However, flakes with smaller sizes can still be seen at this stage, further proving that new seeds have been formed continuously on the exposed Co surface. After the growth is extended to 1800 s, continuous h-BN film is finally formed on most of the Co surface except the edge areas of the sample, where discrete flakes still exist. The single domain boundaries can be easily identified (Figure S2d) and the single domain size can be estimated to be in the

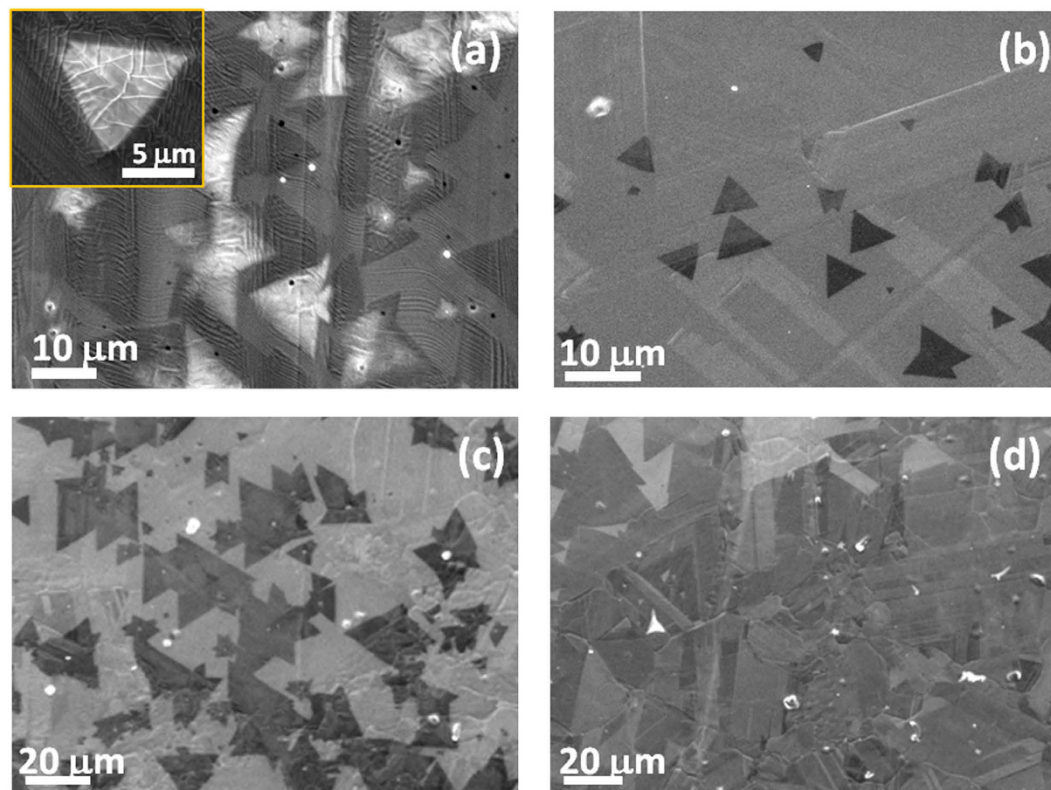


Figure 1. SEM images of h-BN films grown on (a) unpolished foil for 900 s (Sample A), and on polished foils for (b) 450 s (Sample B), (c) 900 s (Sample C) and (d) 1800 s (Sample D). The inset in (a) is a magnified image of an h-BN flake on Sample A.

range of 20~100 μm. H-BN flakes growing across Co grain boundaries are also frequently observed, which suggests that h-BN growth is surface-mediated under these conditions^{19,21}.

In order to assess the surface morphology effect on the nucleation and growth of h-BN, we compare SEM and AFM images of Sample A (Fig. 1a and Figure S3) and Sample C (Fig. 1c and Figure S4), showing h-BN films on unpolished and polished Co foils, respectively, grown under the same growth conditions. In general, the h-BN grown on polished Co foil has larger single-domain size and more uniform thickness, compared with the h-BN grown on unpolished Co foil. It has been proposed that one key approach to grow large, single-crystalline h-BN domains is to reduce the nucleation density at the early stage of growth²⁰. The defects, such as grain boundaries, rough edges, uneven grooves, and impurities on unpolished Co substrates provide relatively lower activation energy for h-BN to nucleate compared with smooth regions³⁶. Since polishing process can remove a large amount of these defects, the nucleation sites are significantly reduced and more evenly distributed on polished Co surfaces. Thus, the h-BN domains grown on polished Co are more uniform in both domain size and thickness, compared with their counterparts on unpolished Co. The low nucleation density decreases the competition for impinging atoms among different seeds locally, which helps maintain the same growth conditions for different seeds. Farther apart seeds grow at the same rate and are evenly spread. After the initial h-BN nucleation, smooth polished Co surface provides lower kinetic energy barrier and longer diffusion length for B and N atoms to diffuse. These atoms with high kinetic energy can diffuse across a large area, and react and settle at the active edges of BN seeds, which continue to grow into large, single-crystalline domains. In contrast, on unpolished Co surfaces with a larger kinetic energy barrier and lower diffusion length caused by rough surface, B and N atoms tend to accumulate locally and form adlayers, rather than diffuse across the barrier. The formation of adlayers can be also associated with defects from rough substrate, which would cause strain in the existing layers, leading to further nucleation on top of the existing layers. Our result proves that it is indeed important to decrease the number of nucleation sites to achieve large domain sizes. In other words, there is a great possibility to achieve high-quality h-BN films with large-size and single-crystalline domains on smooth Co foil substrates.

It is interesting to note that besides regular triangular domains, other complex polygons with well-defined edges are observed as the initial form of h-BN flakes among all samples on polished Co substrates. Figure 2a–e show SEM images of these flakes, and Fig. 2f–j show one-to-one corresponding possible schematic illustrations of their atomic arrangements: triangle shape, “kite” shape, “hourglass” shape, “butterfly” shape and multi-apex-star shape, respectively. From theoretical calculations³⁸, the triangular h-BN domain is single crystal with nitrogen-terminated zigzag edges due to energetic preferences, as shown in Fig. 2a,f. Figure 2b,g show a kite-shape domain composed of two triangles with alternating nitrogen-terminated edges and boron-terminated edges¹⁹. Hourglass-shape domain is composed of two similar quadrangles with nitrogen-terminated edges and

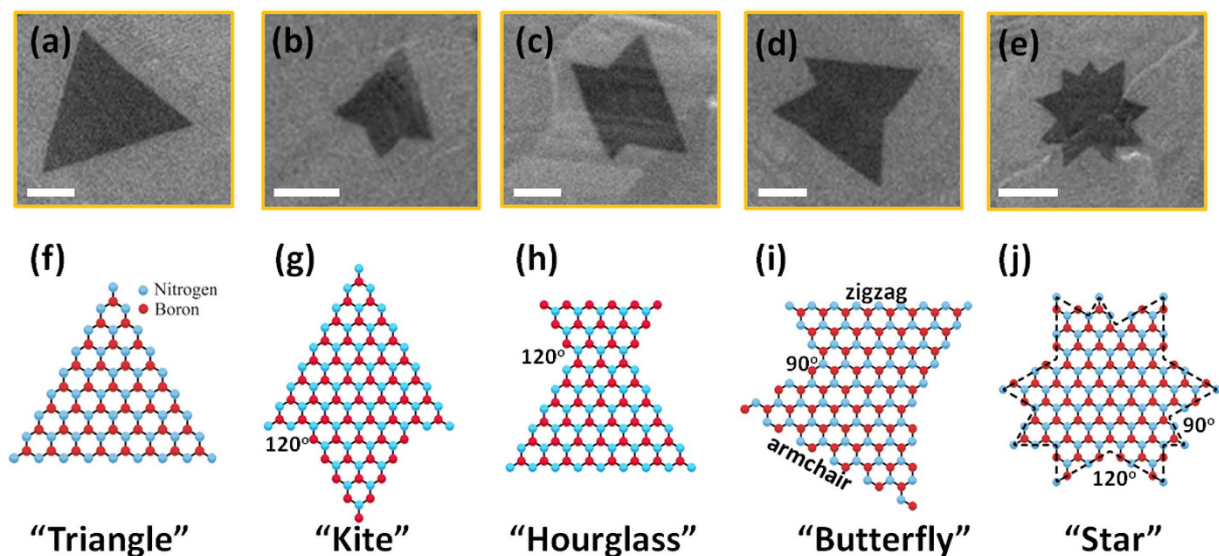


Figure 2. SEM images paired with schematic illustrations of h-BN domains with different atomic arrangements: (a,f) triangle shape, (b,g) “kite” shape, (c,h) “hourglass” shape, (d,i) “butterfly” shape and (e,j) multi-apex-star shape. Scale bars in (a–e) are 5 μm .

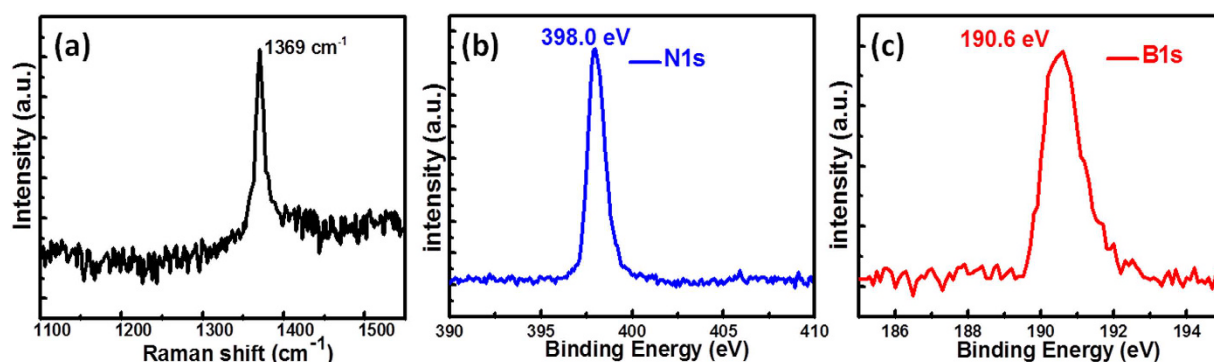


Figure 3. (a) Raman spectrum of as-grown h-BN film (Sample D). XPS spectra of (b) N1s and (c) B1s peaks.

boron-terminated edges, as shown in Fig. 2c,h. In addition, mutually perpendicular edges are observed from butterfly-shape domain (Fig. 2d,i) and multi-apex-star-shape domain (Fig. 2e,j), which indicates the connection of one zigzag edge with a neighboring armchair edge from simple geometry. Although the growth mechanism of complex domain structures remains elusive, the two merging modes, namely, point-to-edge and edge-to-edge modes³⁹ can be a possible explanation. For example, as the nucleation sites are close enough to one another, the coalescence between the domains would occur when they grow larger, resulting in multifaceted shapes.

Based on the continuous film of Sample D, further characterizations have been performed to assess the h-BN. Figure 3a shows Raman spectrum of the as-grown h-BN film. A single peak at 1368 cm^{-1} is assigned to the E_{2g} vibration mode of h-BN²⁰. In addition, the full width at half maximum (FWHM) of this Raman peak is only 11 cm^{-1} , which is indicative of high-crystalline h-BN film³³. XPS spectra in Fig. 3b and c show an evident peak for B 1s and N 1s at 190.6 and 398.0 eV, respectively, further confirming the existence of the B-N bond^{4,11}. The B/N elemental ratio can be extracted as $\sim 1:1.06$ based on the integral intensities of the characteristic peaks, which suggests an almost equal composition of B and N elements.

Figure 4a shows an optical microscopy image of the h-BN film transferred onto a SiO_2/Si substrate, showing a large-size continuous film with a clear contrast from the SiO_2/Si substrate. The surface morphology of the h-BN film was further characterized by AFM, which is shown in Fig. 4b. The height profile of a scanned line indicates that the h-BN has a thickness of 5–6 nm on average for 1800-s growth. It is worth noting that the thickness of the h-BN flakes in Sample C (900-s growth) is estimated to be 2.2 nm (Figure S4), which suggests that h-BN growth may start with nucleation sites of a few layers and then grow into large domains⁴⁰. Considering the thickness and coverage evolution from Sample C to Sample D, it indicates that initial flakes grow laterally as well as vertically into multilayer film as the growth time lapses. Figure 4c shows a plan-view TEM image of the transferred h-BN film. A continuous thin film is observed. The SAED pattern of the h-BN thin film is seen in the inset of Fig. 4c, showing a clear hexagonal set of diffraction spots. The in-plane lattice constant can be estimated as approximately

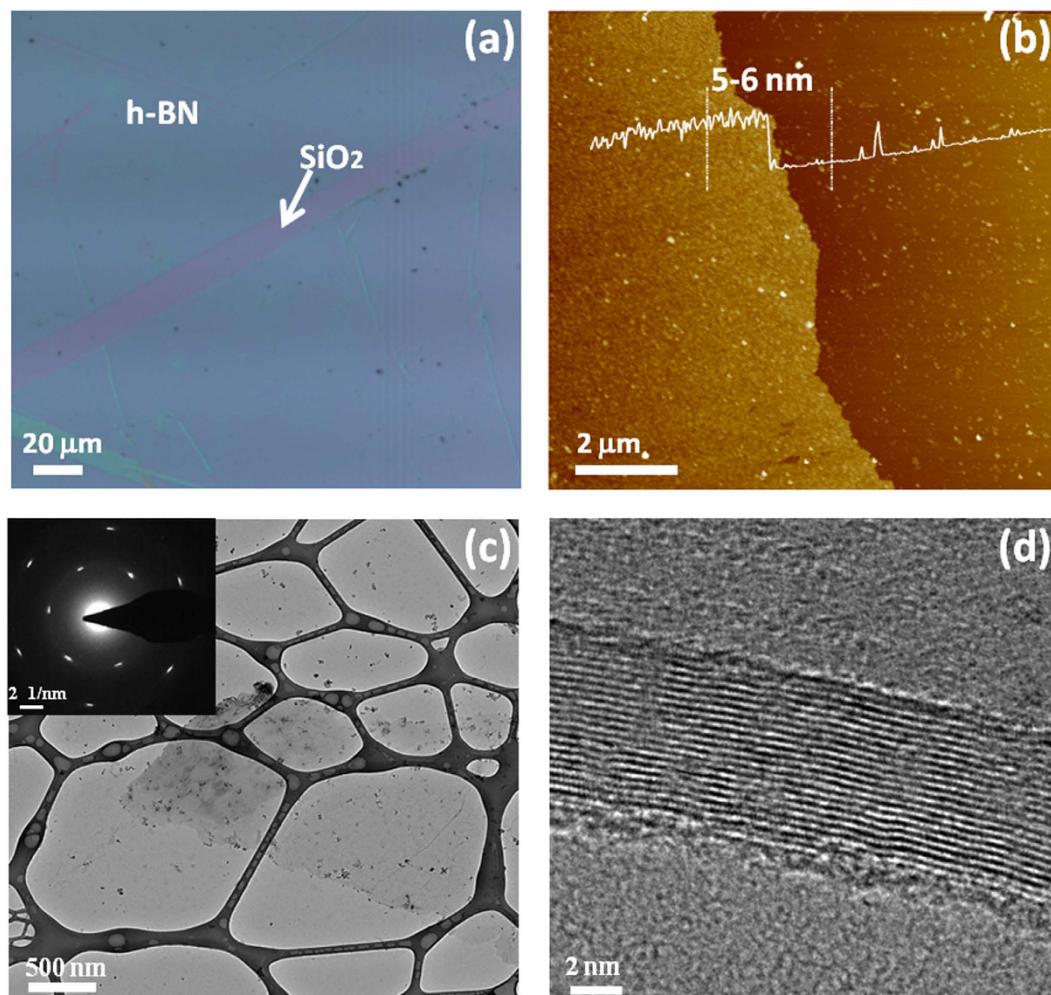


Figure 4. (a) Optical micrograph and (b) AFM image of the transferred h-BN film (Sample D) on SiO₂. (c) Plan-view TEM image of the transferred h-BN film on a carbon-coated Cu TEM grid. Inset is an electron diffraction pattern, showing six-fold symmetry of the h-BN film. (d) High-resolution TEM image showing multi-layer structure of the h-BN film near its edge.

2.47~2.5 Å, which is in good agreement with that of h-BN²². High resolution TEM image (Fig. 4d) shows the lattice fringes of the h-BN film with an interlayer distance of 0.33 nm, which matches previously reported values of h-BN^{11,31}. The thickness is measured to be ~6 nm, which is consistent with the AFM results.

To evaluate the insulating property of the h-BN film, electrical breakdown characterization was performed on Co(foil)/h-BN/Co(metal contact) capacitor devices based on Sample D. Figure 5 shows typical curves of current density versus electric field from square-shaped devices with three different edge lengths of 100, 50, and 20 μm, respectively. The 100-μm device shows significant leakage without any evident breakdown point, which can be originated from pinholes, grain boundaries or significant defects (Figure S2d), leading to a conducting behavior. In contrast, devices with 50-μm and 20-μm edge lengths show much-improved insulating characteristics although there were still many of the tested devices showing similar behavior to that of the 100-μm-sized devices due to the same above-mentioned factors. In addition, it is worth to note that these smaller devices have similar leakage current at lower bias compared with those based on mechanically exfoliated BN films⁴¹. The hard breakdown phenomenon can be observed in the range of 3.0~3.3 MV/cm, which is comparable with the values from the devices based on h-BN films grown by CVD^{8,11,42} and exfoliated h-BN films⁴³. In addition to the vertical electrical characterizations, in-plane electrical characterizations were also carried out on a transferred h-BN thin film of Sample D on SiO₂ (Figure S5). Currents are negligible under a voltage sweep across pairs of separated metal contacts placed on top of the film. These results suggest good insulating characteristics of the h-BN film grown by MBE.

Conclusion

We demonstrated large-area growth of multi-layer h-BN films on mechanically polished Co foils using plasma-assisted MBE. Time-dependent h-BN growth indicates that the coverage of h-BN domains with various polygon shapes on the surface increases as the increase of the growth time. The dielectric properties of as-grown h-BN film with a thickness of 5~6 nm are evaluated by characterization of Co(foil)/h-BN/Co(contact) capacitor

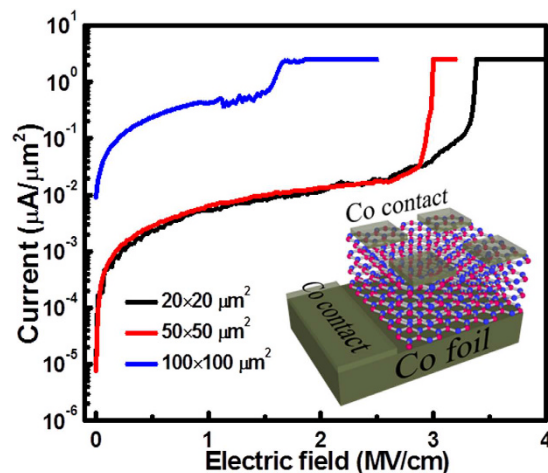


Figure 5. Current density-electric field characteristics of Co(foil)/h-BN/Co(contact) devices with different contact sizes. Inset shows a schematic of the devices.

devices. Breakdown electric field is estimated to be 3.0–3.3 MV/cm, which indicates that the epitaxial h-BN film has good insulating characteristics. In addition, by comparing the results of h-BN growth on unpolished and polished Co foils, it is concluded that the morphology of Co foil surface affects h-BN growth with respect to domain density, lateral size and thickness since the control of the density of nucleation sites plays a key role on the growth of h-BN films.

References

- Nag, A. *et al.* Graphene Analogues of BN: Novel Synthesis and Properties. *ACS Nano* **4**, 1539–1544 (2010).
- Liu, L., Feng, Y. P. & Shen, Z. X. Structural and Electronic Properties of h-BN. *Phys. Rev. B* **68**, 104102 (2003).
- Watanabe, K., Taniguchi, T. & Kanda H. Direct-bandgap properties and evidence for ultraviolet lasing of hexagonal boron nitride single crystal. *Nat. Mat.* **3**, 404–409 (2004).
- Song, L. *et al.* Large Scale Growth and Characterization of Atomic Hexagonal Boron Nitride Layers. *Nano Lett.* **10**, 3209–3215 (2010).
- Dean, C. R. *et al.* Boron nitride substrates for high-quality graphene electronics. *Nat. Nanotechnol.* **82**, 722–726 (2010).
- Levendorf, M. P. *et al.* Graphene and boron nitride lateral heterostructures for atomically thin circuitry. *Nature* **488**, 627–632 (2012).
- Dean, C. R. *et al.* Hofstadter's butterfly and the fractal quantum Hall effect in moiré superlattices. *Nature* **497**, 598–602 (2013).
- Kim, K. K. *et al.* Synthesis and Characterization of Hexagonal Boron Nitride Film as a Dielectric Layer for Graphene Devices. *ACS Nano* **6**, 8583–8590 (2012).
- Lee, K. H. *et al.* Large-scale synthesis of high-quality hexagonal boron nitride nanosheets for large-area graphene electronics. *Nano Lett.* **12**, 714–718 (2012).
- Britnell, L. *et al.* Field-Effect Tunneling Transistor Based on Vertical Graphene Heterostructures. *Science* **335**, 947–950 (2012).
- Kim, S. M. *et al.* Synthesis of large-area multilayer hexagonal boron nitride for high material performance. *Nat. Commun.* **6**, 8662 (2015).
- Yan, A. *et al.* Direct growth of single- and few-layer MoS₂ on h-BN with preferred relative rotation angles. *Nano Lett.* **15**, 6324–6331 (2015).
- Wang, S., Wang, X. & Warner, J. H. All Chemical Vapor Deposition Growth of MoS₂:h-BN Vertical van Der Waals Heterostructures. *ACS Nano* **9**, 5246–5254 (2015).
- Okada, M. *et al.* Direct Chemical Vapor Deposition Growth of WS₂ Atomic Layers on Hexagonal Boron Nitride. *ACS Nano* **8**, 8273–8277 (2014).
- Behura, S., Nguyen, P., Che, S., Debbarma, S. & Berry, V. Large-Area, Transfer-Free, Oxide-Assisted Synthesis of Hexagonal Boron Nitride Films and Their Heterostructures with MoS₂ and WS₂. *J. Am. Chem. Soc.* **137**, 13060 (2015).
- Wang, L., Wu, B., Chen, J., Liu, H., Hu, P. & Liu, Y. Monolayer Hexagonal Boron Nitride Films With Large Domain Size and Clean Interface for Enhancing The Mobility of Graphene-Based Field-Effect Transistors. *Adv. Mater.* **26**, 1559–1564 (2014).
- Novoselov, K. S. *et al.* Two-Dimensional Atomic Crystals. *Proc. Natl. Acad. Sci. USA* **102**, 10451–10453 (2005).
- Coleman, J. N. *et al.* Two-Dimensional Nanosheets Produced by Liquid Exfoliation of Layered Materials. *Science* **331**, 568–571 (2011).
- Kim, K. K. *et al.* Synthesis of Monolayer Hexagonal Boron Nitride on Cu Foil Using Chemical Vapor Deposition. *Nano Lett.* **12**, 161–166 (2011).
- Tay, R. Y. *et al.* Growth of large single-crystalline two-dimensional boron nitride hexagons on electropolished copper. *Nano Lett.* **14**, 839–846 (2014).
- Wang, H. *et al.* Controlled Growth of Few-layer Hexagonal Boron Nitride on Copper Foils Using Ion Beam Sputtering Deposition. *Small* **11**, 1542–1547 (2015).
- Shi, Y. M. *et al.* Synthesis of Few-layer Hexagonal Boron Nitride Thin Film by Chemical Vapor Deposition. *Nano Lett.* **10**, 4134–4139 (2010).
- Ismach, A. *et al.* Toward the Controlled Synthesis of Hexagonal Boron Nitride Films. *ACS Nano* **6**, 6378–6385 (2012).
- Caneva, S. *et al.* Controlling Catalyst Bulk Reservoir Effects for Monolayer Hexagonal Boron Nitride CVD. *Nano Lett.* **16**, 1250–1261 (2016).
- Sutter, P., Lahiri, J., Zahl, P., Wang, B. & Sutter, E. Scalable synthesis of uniform few-layer hexagonal boron nitride dielectric films. *Nano Lett.* **13**, 276–281 (2012).
- Kim, G. *et al.* Growth of High-Crystalline, Single-Layer Hexagonal Boron Nitride on Recyclable Platinum Foil. *Nano Lett.* **13**, 1834–1839 (2013).
- Gao, Y. *et al.* Repeated and Controlled Growth of Monolayer, Bilayer and Few-Layer Hexagonal Boron Nitride on Pt Foils. *ACS Nano* **7**, 5199–5206 (2013).

28. Glavin, N. R. *et al.* Synthesis of Few-Layer, Large Area Hexagonal-Boron Nitride by Pulsed Laser Deposition. *Thin Solid Films* **572**, 6–11 (2014).
29. Meng, J. H. *et al.* Synthesis of in-plane and stacked graphene/hexagonal boron nitride heterostructures by combining with ion beam sputtering deposition and chemical vapor deposition. *Nanoscale* **7**, 16046–16053 (2015).
30. Zhang, C. H. *et al.* Direct growth of large-area graphene and boron nitride heterostructures by a co-segregation method. *Nat. Commun.* **6**, 6519 (2015).
31. Zhang, C., Fu, L., Zhao, S., Zhou, Y., Peng, H. & Liu, Z. Controllable Co-Segregation Synthesis of Wafer-Scale Hexagonal Boron Nitride Thin Films. *Adv. Mater.* **26**, 1776–781 (2014).
32. Xu, Z., Zheng, R., Khanaki, A., Zuo, Z. & Liu, J. Direct growth of graphene on *in situ* epitaxial hexagonal boron nitride flakes by plasma-assisted molecular beam epitaxy. *Appl. Phys. Lett.* **207**, 213103 (2015).
33. Nakhaie, S. *et al.* Synthesis of atomically thin hexagonal boron nitride films on nickel foils by molecular beam epitaxy. *Appl. Phys. Lett.* **106**, 213108 (2015).
34. Tonkikh, A. A. *et al.* Structural and electronic properties of epitaxial multilayer h-BN on Ni(111) for spintronics applications, *Sci. Reps.* **6**, 23547 (2016).
35. Zuo, Z., Xu, Z., Zheng, R., Khanaki, A., Zheng, J. & Liu, J. *In-situ* epitaxial growth of graphene/h-BN van der Waals heterostructures by molecular beam epitaxy. *Sci. Rep.* **5**, 14760 (2015).
36. Khan, M. H. *et al.* Synthesis of large and few atomic layers of hexagonal boron nitride on melted copper. *Sci. Rep.* **5**, 7743 (2015).
37. Oliveira, C. K. *et al.* Crystal-oriented wrinkles with origami-type junctions in few-layer hexagonal boron nitride. *Nano Res.* **8**, 1680–1688 (2015).
38. Liu, Y., Bhowmick S. & Yakobson, B. BN White Graphene with “Colorful” Edges: The Energies and Morphology. *Nano Lett.* **11**, 3113–3116 (2011).
39. Wang, L. *et al.* Growth and Etching of Monolayer Hexagonal Boron Nitride. *Adv. Mater.* **27**, 4858–4864 (2015).
40. Tay, R. Y. *et al.* Systematic Study of the Atmospheric Pressure Growth of Large-Area Hexagonal Crystalline Boron Nitride Film. *J. Mater. Chem. C* **2**, 1650–1657 (2014).
41. Britnell, L. *et al.* Electron Tunneling through Ultrathin Boron Nitride Crystalline Barriers. *Nano Lett.* **12**, 1707–1710 (2012).
42. Bresnehan, M. S., Bhimanapati, G. R., Wang, K., Snyder, D. W. & Robinson, J. A. Impact of Copper Overpressure on the Synthesis of Hexagonal Boron Nitride Atomic Layers. *ACS Appl. Mater. Interfaces* **6**, 16755–16762 (2014).
43. Lee, G.-H. *et al.* Electron tunneling through atomically flat and ultrathin hexagonal boron nitride. *Appl. Phys. Lett.* **99**, 243114 (2011).

Acknowledgements

This work was supported by FAME, one of six centers of STARnet, a Semiconductor Research Corporation program supported by MACRO and DARPA.

Author Contributions

J.L. leads the project. Z.X. designed and performed the epitaxial growth. H.T. contributed on schematic drawing and electrical measurement. Z.X., H.T. and A.K. performed SEM imaging and analysis. R.Z. and Z.X. performed TEM imaging and analysis. M.S. contributed to fabricated capacitor devices. Z.X. and J.L. wrote the manuscript. All authors contributed to analyzing and reviewing the data in this manuscript.

Additional Information

Supplementary information accompanies this paper at <http://www.nature.com/srep>

Competing financial interests: The authors declare no competing financial interests.

How to cite this article: Xu, Z. *et al.* Large-area growth of multi-layer hexagonal boron nitride on polished cobalt foils by plasma-assisted molecular beam epitaxy. *Sci. Rep.* **7**, 43100; doi: 10.1038/srep43100 (2017).

Publisher's note: Springer Nature remains neutral with regard to jurisdictional claims in published maps and institutional affiliations.



This work is licensed under a Creative Commons Attribution 4.0 International License. The images or other third party material in this article are included in the article's Creative Commons license, unless indicated otherwise in the credit line; if the material is not included under the Creative Commons license, users will need to obtain permission from the license holder to reproduce the material. To view a copy of this license, visit <http://creativecommons.org/licenses/by/4.0/>

© The Author(s) 2017